Organic & Biomolecular Chemistry

Accepted Manuscript

This article can be cited before page numbers have been issued, to do this please use: R. Booth, I. Insua, G. Bhak and J. Montenegro, *Org. Biomol. Chem.*, 2018, DOI: 10.1039/C8OB02243G.

ROYAL SOCIETY OF CHEMISTRY

rsc.li/obc

View Article Online
DOI: 10.1039/C8OB02243G

Journal Name

PAPER

Self-Assembled Micro-Fibres by Oxime Connection of Linear Peptide Amphiphiles

Received 00th January 20xx,

Accepted 00th January 20xx

DOI: 10.1039/x0xx00000x

www.rsc.org/

Richard Booth, Ignacio Insua, Ghibom Bhak and Javier Montenegro*

Linear peptide amphiphiles are excellent biocompatible scaffolds for the hierarchical self-assembly of one dimensional nano-structures in aqueous media. However, their structural exploration and screening of self-assembling properties is often limited by time-consuming synthesis and purification steps. We here describe the application of the oxime bond as a powerful synthetic tool towards the conjugation of peptide heads bearing a hydroxylamine group with hydrophobic aldehyde tails. This methodology allowed the quick prepraration of a small library of oxime-connected peptide amphiphiles, whose supramolecular screening revealed nano-to-micro fibrillation with dependency on their chemical structure. These results demonstrate the simplicity and the synthetic potential of the oxime conjugation for the preparation of peptide amphiphiles with improved self-assembling capabilities.

Introduction

Peptide amphiphiles are short peptide sequences in which the thermodynamic incompatibility of different moieties imparts spatial organization into a range of morphologies (*e.g.* nanofibers, vesicles, *etc.*).[1-4] Such behaviour has been applied in the development of artificial confined supramolecular assemblies,[5] membrane transporters,[6,7] stimuli-responsive soft materials[8,9] and novel semi-conducting materials.[10,11] One type of amphiphilic peptides consist of a short linear hydrophilic peptide scaffold with amphiphilicity provided by the attachment of an aliphatic tail.[12-20] In these linear peptide amphiphiles, the peptide sequence generally consists of a hydrophilic charged head to aid solubility, and a β-sheet forming region close to a final aliphatic chain of lengths between ten and fourteen carbon atoms.[21,22] In water, the β-sheet promoting sequences of the peptides, coupled with the collapse of the hydrophobic tail induce self-assembly into nanostructures, most commonly cylindrical or ribbon-like nanofibers.[23,24] These supramolecular structures hold great promise for therapeutic biomedical applications due to their inherent biocompatible and biodegradable nature, together with the ability to carefully design the peptide sequence for specific bioactive functions.[25-38] Careful choice of the peptide sequence can also alter the non-covalent interactions driving self-assembly and hence allow the engineering of peptide amphiphiles with a range of structures and properties, including closed sacs,[39] aligned fibres,[40] nanobelts[41] and micelles.[42]

Currently, the synthesis of these type of peptide amphiphiles is commonly achieved by using standard solid phase peptide synthesis, including the final addition of the aliphatic tail; a synthetic procedure that demands a fresh synthesis for each peptide amphiphile. In this regard, an optimized method for the quick production of large libraries of peptide amphiphiles would facilitate the identification of the best potential structures for controlled self-assembly under different conditions. The employment of dynamic covalent chemistry such as hydrazones,[43-45] hydrazides,[46] oximes[47-49] and disulphides[50] can allow the screening of a large number of potential targets in supramolecular chemistry and chemical biology. These dynamic bonds react quickly, with high yields and with no by-products. In addition, dynamic covalent chemistry and related techniques are sensitive to external stimuli[51,52] and could enable the development of peptide amphiphiles that adapt to changes in the external environment, potentially leading to supramolecular structures with enhanced properties applicable to regenerative medicine

[a] *Centro Singular de Investigación en Química Biolóxica e Materiais Moleculares (CIQUS), Departamento de Química Orgánica, Universidade de Santiago de Compostela, 15782 Santiago de Compostela, Spain. *e-mail: javier.montenegro@usc.es*

Electronic Supplementary Information (ESI) available: [details of any supplementary information available should be included here]. See DOI: 10.1039/x0xx00000x.

View Article Online
DOI: 10.1039/C8OB02243G

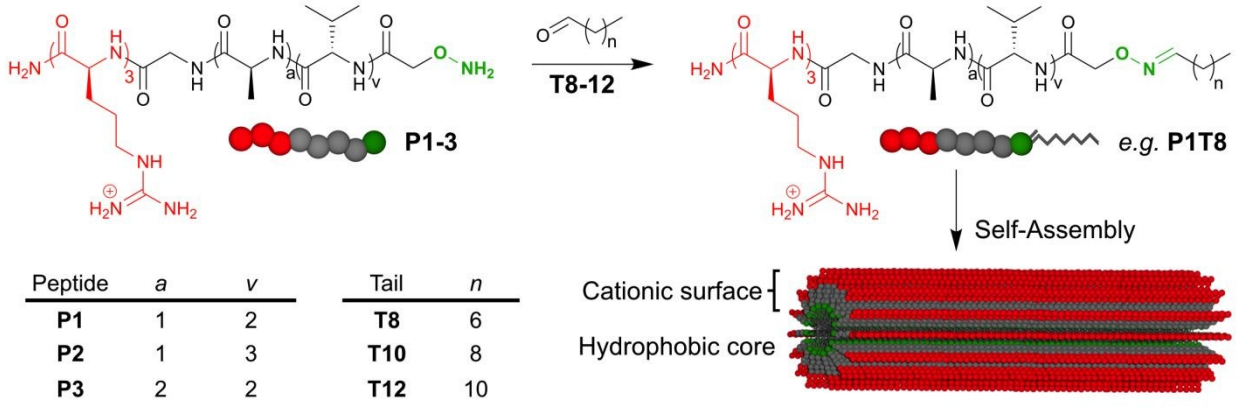

Peptide	a	v	Tail	n
P1	1	2	**T8**	6
P2	1	3	**T10**	8
P3	2	2	**T12**	10

Fig. 1. Schematic representation of the cationic arginine-based (red region) peptide amphiphiles synthesized by an oxime connection (green region) to aliphatic aldehydes and their subsequent self-assembly into peptide fibres. *Note that peptide sequences and structures are drawn from *C* to *N*-terminus throughout the paper for clarity in the synthetic schemes.

or drug delivery systems.[53,54] As discussed previously, linear peptide amphiphiles tend to self-assemble into cylindrical peptide fibres on the nanoscale.[2,4] However, depending on the conditions, not all of these nano-structures are capable of maintaining the hierarchical longitudinal ordering on the micron scale after bundling or aggregating. Nevertheless, the bundling of nano-assemblies into fibrillated micron-sized structures is one of the hallmarks of cytoskeleton forming proteins in living systems.[5,55] This hierarchical assembly allows the transduction of the nano-assembly into strong physical forces capable of triggering complex biological functions such as chemotaxis and cell division.[56,57] In this regard, the development of synthetic tools that would allow the quick and efficient synthesis of linear peptide amphiphiles would simplify the preparation and identification of self-assembled fibrillated structures on the micron scale and at physiologically compatible conditions. Additionally, the development of such a method would contribute to the identification of simple fibrillating peptide amphiphiles that could be potentially employed in biology, medicine and in bottom-up approaches to synthetic biology.

In this paper, we aimed to employ an oxime bond forming reaction as a tool to synthesize peptide amphiphiles containing aliphatic tails of varying lengths, and to identify potential structures capable of forming fibres on the micron scale. The use of a hydroxylamine functional group on the *N*-terminus of the peptide allowed the facile conjugation of short peptide sequences with a range of aliphatic chains (**Fig. 1** and **Fig. 3**). The library of synthesized amphiphiles was screened for their self-assembly properties and fibrillation on the micron-scale by fluorescence microscopy using a planarizable fluorescent probe. Cationic and anionic peptide amphiphiles were produced and both were found to self-assemble into micron-sized fibres over a range of external conditions and timescales, signifying how small changes in structure can dramatically affect self-assembly properties. Our results highlight the advantage of using dynamic covalent chemistry as a synthetic tool to rapidly access collections of peptide amphiphiles for supramolecular and self-assembly screening.

Results and Discussion

Oxime connection to produce cationic (arginine) peptide amphiphiles

In order to quickly and efficiently synthesise a range of peptide amphiphiles (PAs) with potential self-assembly properties, peptide heads were synthesised using standard solid-state peptide synthesis techniques (see experimental section) with a hydroxylamine functional group (-ONH_2) for subsequent connection with a range of aliphatic aldehydes of different lengths (**Fig. 1**). Once synthesised and characterised (supporting information), the peptide heads were reacted with the corresponding aldehyde aliphatic chains (DMSO, 60 °C, 1 h) to afford PAs quantitatively in a facile and efficient manner. The basic structure of these PAs consisted of a cationic *C*-terminus of 3 L-arginine groups, a hydrogen bond β-sheet promoting centre region which consisted of alanine and valine amino acids and a hydroxylamine group at the *N*-terminus (**Fig. 1**). One example of the cationic series of these peptide heads consisted of the sequence R_3GAV_2 functionalized with *O*-(carboxymethyl)hydroxylamine (**P1**), which was subsequently reacted with aliphatic aldehydes (**T8**-**T12**) to yield the corresponding peptide amphiphiles (**P1T8**-**T12**, **Fig. 1**). After the oxime bond connection, the peptide amphiphile was precipitated in diethyl ether and washed extensively with the same solvent. Thus, the obtained amphiphiles did not require any further purification and could be characterized by HPLC-MS and HRMS (see supporting information). All conjugation reactions between peptide heads and aldehyde tails went to completion according to HPLC analysis, and the final isolated yields were excellent (~90%).

For the self-assembly studies, we prepared aqueous solutions (10 $mg{\cdot}mL^{-1}$) of these peptide amphiphiles in Tris-HCl buffer (50 mM,

View Article Online
DOI: 10.1039/C8OB02243G

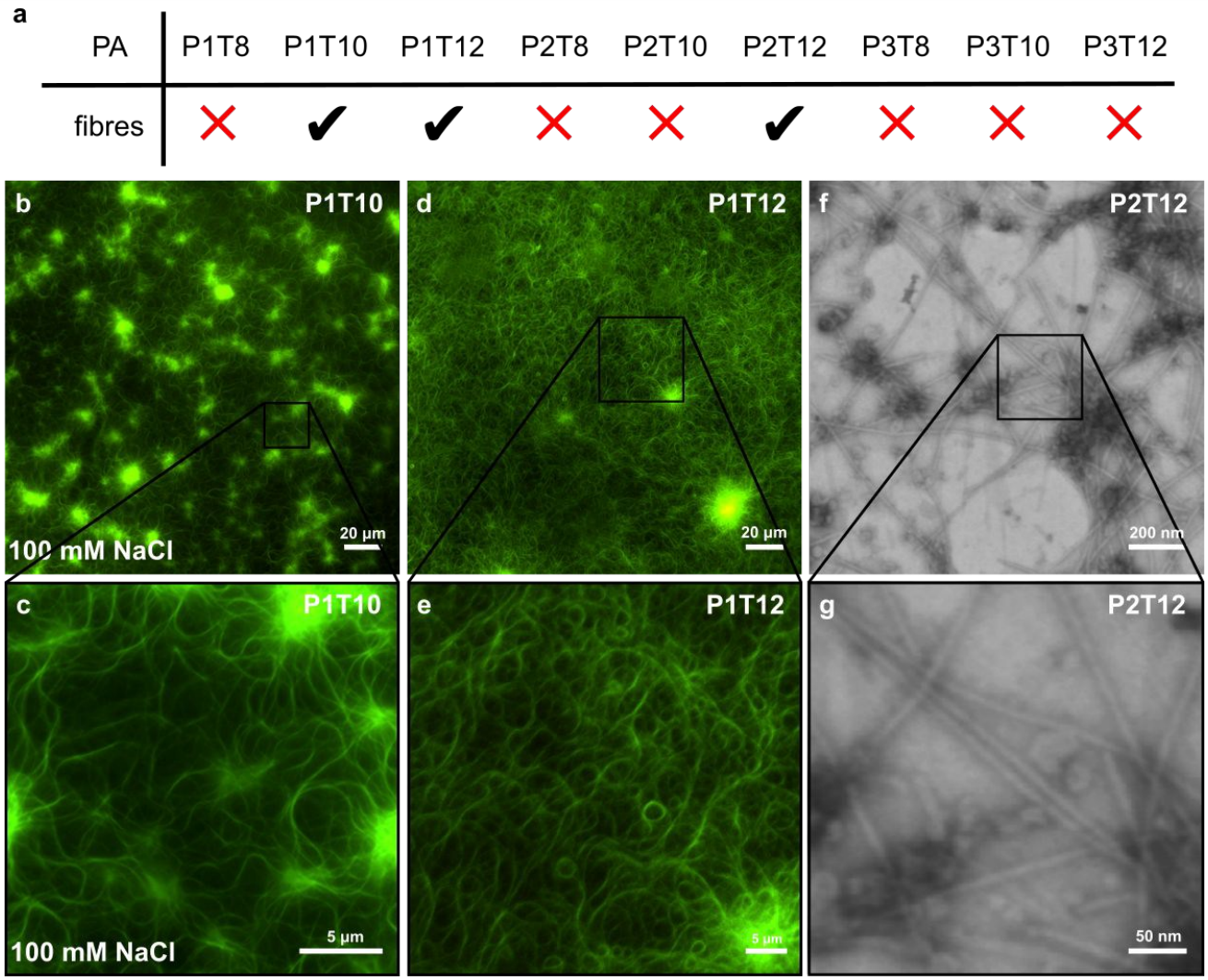

Fig. 2. (**a**) Table of the cationic arginine-based peptide amphiphiles synthesised in this study and whether fibres were observed. (**b-e**) Fluorescence microscopy of micron-sized peptide amphiphile fibres at 10 mg·mL^{-1} (50 mM Tris-HCl, pH 7.5) after 16 h incubation of **P1T10** with 100 mM NaCl (**b**), at increased magnification (**c**), of **P1T12** in buffer with no NaCl (**d**) and at increased magnification (**e**). (**f,g**) STEM images of **P2T12** peptide nano-sized fibres (50 mM Tris-HCl, pH 7.5) after 16 h incubation (**f**) and at increased magnification (**g**).

pH 7.5) and studied their properties by fluorescence microscopy. All of the peptide amphiphiles were first sonicated for 1 h at 60 °C to dissolve the amphiphile, breaking up any pre-formed aggregates prior to studying self-assembly. The fluorescent dye thioflavin T (5 μM) was added to the solutions to image them by epifluorescence microscopy. No microfibre formation was apparent in **P1T8**, presumably due to the higher solubility of this amphiphile. However, micron-sized fibres were visible in samples of **P1T10** and **P1T12** after approximately 16 h (**Figs. 2 and S40**). Some of the formed fibres had small diameters and so were harder to distinguish by optical microscopy (*e.g.* **P1T10**, **Fig. S40**). To promote the aggregation of these PAs into fibres, NaCl (100 mM) was added to shield the electrostatic repulsion between guanidinium groups present in these peptide heads (**P1**-**3**), which could hamper self-assembly. Indeed, the addition of NaCl produced more discernible fibres in the **P1T10** sample (**Fig. 2b,c**) but caused aggregated bundles instead of fibre-like structures in the more hydrophobic **P1T12** peptide amphiphile (**Fig. S41**). The formed fibres in both **P1T10** (100 mM NaCl) and **P1T12** (no NaCl) had diameters in the order of 200-400 nm (280 ± 50 nm and 320 ± 50 nm, respectively), which were clearly distinguishable by fluorescence microscopy (**Fig. 2b-e**).

In addition to the previously discussed peptide head, two more peptide heads were synthesised with slights variations in the β-sheet seed region, namely **P2** and **P3**, containing an AVVV or an AAVV centre sequence, respectively (**Fig. 1**). Again, no fibre formation was apparent immediately after sample preparation,

View Article Online
DOI: 10.1039/C8OB02243G

nonetheless, when **P2T12** was left for approximately 16 h, high fluorescence was observed but no clear micron-sized individual fibres were found in the fluorescence micrographs (**Fig. S42a**). However, over time (48 hours) thicker individual fibres were observed under the epifluorescence microscope (**Fig. S42b**). This high fluorescence, known to arise from the interaction of thioflavin T with the β-sheets[58] of the self-assembled peptide amphiphiles, could indicate the presence of self-assembled nano-fibres not discernible by optical microscopy. STEM images were acquired after a 16 h incubation of **P2T12**, which revealed the presence of the expected nanofibers of 10 ± 2 nm in diameter (**Fig. 2f,g**). These images suggested that peptide microfibres consisted of nanofibers that aggregate over time, whose kinetics of aggregation can be influenced by both the structure of their constituent peptide amphiphiles and external conditions (*i.e.* ionic strength).

It is important to note that although **P1T12**, bearing the sequence GAVV, was found to fibrillate in the micron scale, the very similar amphiphile **P2T12,** with a slightly longer GAVVV sequence, only exhibited nanotubes and not microfibres. This result suggests that a fine control over hydrophobicity and the sterics are critical for the hydrogen bond-promoting region for fibrillation, which could affect PA packing and ultimately self-assembly. It should also be pointed out that fibrillation of these cationic PAs was sensitive to small variations in the experimental conditions (i.e. peptide concentration, chemical composition of the surface used for self-assembly, ionic strength, etc.). The positively charged character of these structures, their electrostatic attraction to the glass surface and their possible accumulation at the air/water interface might contribute to the sensitivity of the arginine-based PAs (**Fig. S43**).[59]

Oxime connection to produce anionic (glutamic acid) peptide amphiphiles

To further explore the scope of this method for the preparation of self-assembling peptide amphiphiles, a range of anionic peptide heads containing glutamic acid residues were produced in the same manner as discussed previously (**P4**-**6**, **Fig. 3**). The basic structure of these anionic heads was similar to that of the previous arginine-based heads (**P1**-**3**), but in this case we replaced the three arginines for two glutamic acids at the *C*-terminus. The reduction from three ionic residues (**P1**-**3**) to two (**P4**-**6**) was designed to increase the hydrophobicity of the latter peptide heads, potentially leading to a stronger tendency to self-assemble and thus faster fibrillation. The new peptide heads still contained the hydroxylamine functional group required to quickly and efficiently conjugate aliphatic aldehyde tails. The anionic peptides synthesised included the same basic structure in the centre portion as the previous arginine-based peptides (GAVV, **P4**), and two new sequences with increasing hydrogen bond-promoting character (AAVV, **P5** and AAAVV, **P6**). Additionally, to further push and accelerate micron fibre assembly, we decided to increase the length of the hydrophobic tail and incorporate tetradecanal to the tail series (**T14**).

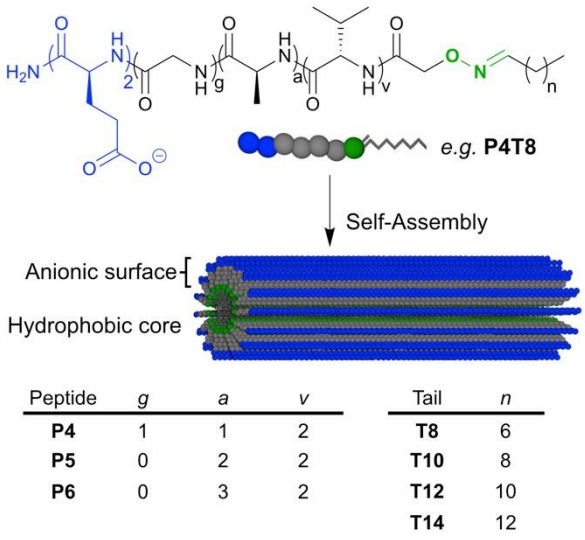

Peptide	*g*	*a*	*v*	Tail	*n*
P4	1	1	2	**T8**	6
P5	0	2	2	**T10**	8
P6	0	3	2	**T12**	10
				T14	12

Fig. 3. Schematic representation of the anionic glutamate-based (blue region) peptide amphiphiles synthesised by an oxime connection (green region) to aliphatic aldehydes and their subsequent self-assembly into peptide fibres. *Note that peptide sequences and structures are drawn from *C* to *N*-terminus throughout the paper for clarity in the synthetic schemes.

Initially, the anionic peptide amphiphiles were dissolved in aqueous solutions at 10 mg·mL^{-1} and their self-assembly properties studied with or without NaCl (100 mM) by fluorescence microscopy. However, fluorescence microscopy revealed only heterogeneous aggregation and no micron-sized fibres were observed under these conditions (**Fig. S44**). In order to decrease their tendency to aggregate and to easily allow full dissolution of the amphiphiles, the peptide amphiphile concentration was lowered to ~ 0.5 mg·mL^{-1} and a range of different ionic strengths was used to identify fibre formation. These optimised conditions (100 mM HEPES, pH 7.5, 100 mM NaCl and 10 mM $MgCl_2$) allowed the self-assembly of **P4T14** and **P5T14** into clear fibre-like structures (**Fig. 4b-e**). However, the remaining anionic amphiphiles either did not assemble on the micron scale or formed disordered aggregates (**Fig. S45**). The anionic fibres self-assembled faster than their arginine-based analogues (**Fig. 1**), producing in less than 1 h, large fibres of around 350-600 nm in diameter (**P4T14** = 500 ± 100 nm and **P5T14** = 450 ± 90 nm). The best amphiphiles for microfibre formation consisted of GAVV (**P4**) or AAVV (**P5**) in the hydrogen bond-promoting centre segment, coupled with the longest and most hydrophobic aldehyde, **T14**. This may be because shorter tails produce amphiphiles that are too soluble or not able to collapse in aqueous solution to promote fibre formation. This is further indicated by the lack of fibre-like

View Article Online
DOI: 10.1039/C8OB02243G

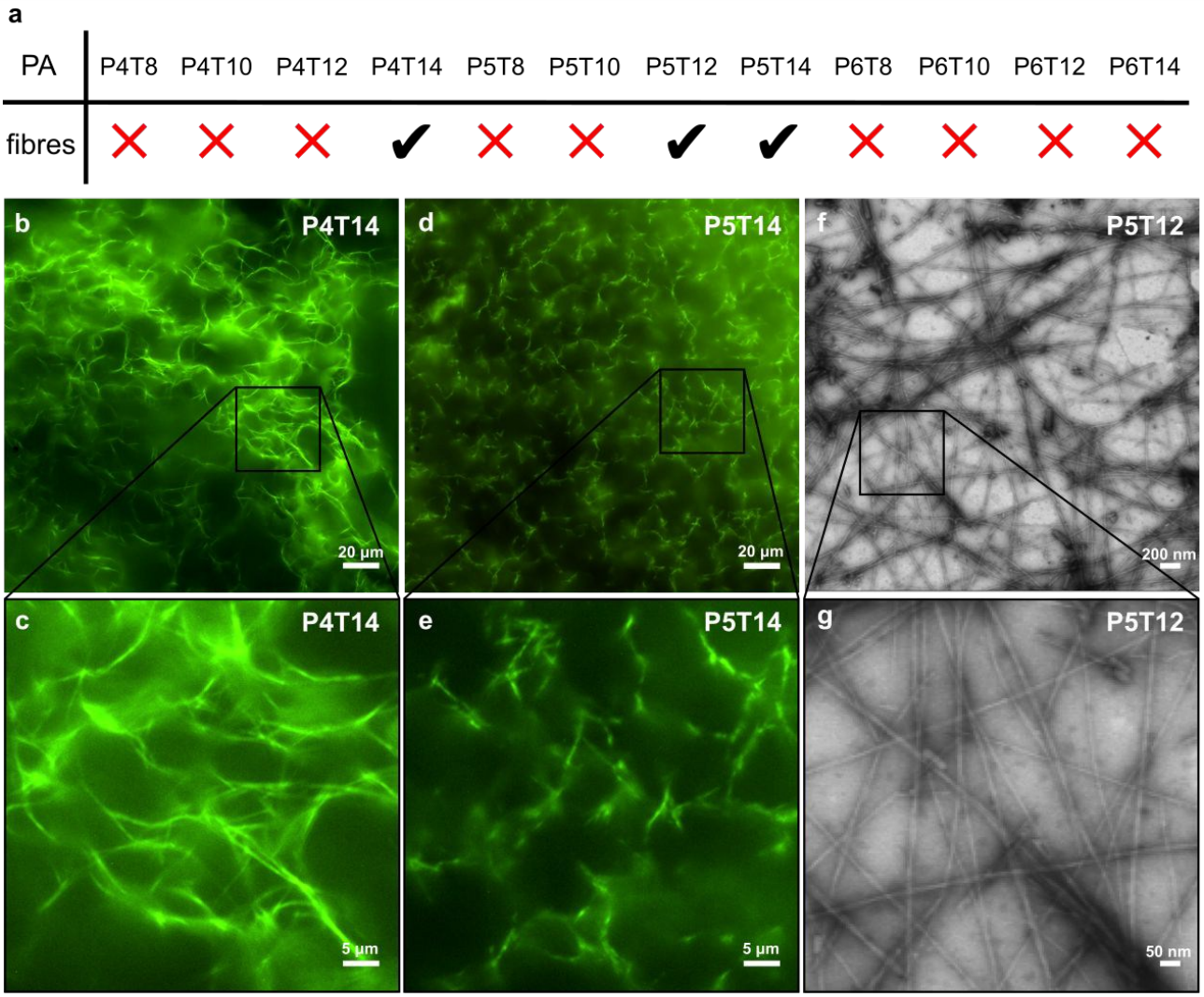

Figure 4. (**a**) Table of the anionic glutamate-based peptide amphiphiles synthesised in this study and whether fibres were observed. (**b-e**) Fluorescence microscopy images of micron-sized peptide amphiphile fibres (0.4 mg·mL^{-1}) after 1 h incubation in aqueous solution (HEPES 100 mM, pH 7.5, 100 mM NaCl, 10 mM $MgCl_2$) of **P4T14** (**b**), at increased magnification (**c**), of **P5T14** (**d**) and at increased magnification (**e**). (**f,g**) STEM images of **P5T12** peptide nano-sized fibres (HEPES 100 mM, pH 7.5, 100 mM NaCl, 10 mM $MgCl_2$) after 10 min incubation (**f**) and at increased magnification (**g**).

structures in samples of **P5T8,** even under a range of experimental conditions (pH, $MgCl_2$ concentration, **Fig. S46**). In addition, too much hydrogen-bonding propensity (AAAVV, **P6**) was found to cause disorganised aggregation (**Fig. S45**). The self-assembly of **P4T14** and **P5T14** consistently produced micron-sized fibres even at elevated temperature and across a range of pH values (**Fig. S47**).

The self-assembly process of the anionic peptide amphiphiles was also studied by STEM microscopy, samples were prepared under the optimised conditions discussed previously (100 mM HEPES, pH 7.5, 100 mM NaCl and 10 mM $MgCl_2$) and were left to self-assemble on carbon-coated copper grids for 10 min. As expected, the STEM images revealed the presence of the nano-sized fibres for the two fibrillating peptides **P4T14** and **P5T14** with diameters of around 10 nm, which were between 30-45 times smaller than the previously measured microfibres (**Fig. S48**). The samples were placed on the carbon-coated copper grids immediately after sonication, therefore the presence of nanofibers in both **P4T14** and **P5T14** indicates that initially nano-sized fibres are present and these subsequently aggregate over time into micron-sized fibrillar bundles (**Figs. 4b-e and S47**). In addition, **P5T12**, which had only shown high fluorescence and no discernible fibres by optical microscopy, was also found to display nano-sized fibres by STEM of 10 ± 2 nm in diameter (**Fig. 4f,g**). This observation confirmed the presence of nano-objects with a much lower

View Article Online
DOI: 10.1039/C8OB02243G

propensity to assemble into fibre-like aggregates for **P5T12** (**Fig. S49**). These results demonstrate that the **T12** tail was not sufficient for producing micron-sized fibres but instead exhibited nano-sized fibre formation with little propensity to aggregate into micron-sized fibrillar bundles. In contrast, **P5T14** self-assembles into microfibres of 360-540 nm in diameter in less than 1 h under the same conditions, showing that a small variation in hydrophobic tail length can lead to large differences in structural self-assembly and can enable the transition from the nano to the micron scale. Finally, to investigate whether non-self-fibrillating PAs could form fibres aided by electrostatic attraction, mixtures of positively charged **P1T8** and negatively charged **P4T8**, with matching H-bonding regions and hydrophobic tails, were mixed together and studied by fluorescence microscopy. None of the mixtures tested showed any sign of fibrillation (**Fig. S50**), reinforcing the idea that fibrillation was dependent on the structure of these PAs (i.e. right peptide sequence and tail length).

Conclusions

These results demonstrate how an oxime connection can be used to facilitate the synthesis of an assortment of peptide amphiphiles with different structures and kinetics of self-assembly. Several oxime-connected peptide amphiphiles based on L-arginine amino acids at the *C*-terminus produced micron-sized fibres of 200-400 nm in diameter after a period of approximately 16 h, which differed from the anionic PAs, which produced fibres that were larger and thicker (350-600 nm in diameter) and on a much quicker timescale of less than 1 h. Our results also demonstrate that it is critical to finely control the central hydrogen bond-promoting sequence of these peptide amphiphiles to achieve fibrillation, as small structural variations have shown to affect supramolecular self-assembly. No fibre formation was ever observed in amphiphiles containing a **T8** aliphatic tail, which suggests that this short tail is not enough to promote the required hydrophobic interactions needed for fibre formation.[60] We also demonstrate that by only changing the length of the alkyl chain, fibres can be produced on both the nano and the micron scale potentially leading to interconvertible structures with distinct properties. In this paper we wanted to highlight the synthetic potential of the oxime connection to screen a large number of potential self-assembling peptide amphiphiles and thus reduce the required synthetic effort to produce peptide fibres on both the nano and micron scale. This method could potentially be used to produce libraries of amphiphiles and identify micro-fibrillating peptides with different properties such as viscoelasticity, or with divergent kinetics of fibre formation. This synthetic strategy could be implemented to produce a range of self-assembling peptide amphiphiles with potential applications as novel therapeutics for tissue engineering,[61] regenerative medicine[62] and drug delivery systems.[63]

Experimental

Peptide head (P1-6) synthesis

Peptide heads were synthesised using Fmoc-Rink Amide AM resin (0.74 mmol·g^{-1}) using standard solid phase peptide synthesis conditions. For each coupling, 4 equiv of the Fmoc protected amino acid were added using 4 equiv of *N*-HBTU and 6 equiv of DIEA in DMF (*N*-HBTU = *N*-[(1H-Benzotriazol-1-yl)-(dimethylamino)methylene]-*N*-methylmethanaminium hexafluorophosphate; DIEA = *N*,*N*-diisopropylethylamine). The Fmoc protecting group was removed each time using 20% piperidine in DMF. The hydroxylamine was added in the last step of the synthesis of each peptide using 2.5 equiv of TBCA, 2.5 equiv of *N*-HATU and 2.5 equiv of DIEA (TBCA = [(tert-Butoxycarbonyl)-aminooxy]acetic acid); *N*-HATU = *N*-[(Dimethylamino)-1*H*-1,2,3-triazolo[4,5-b]pyridin-1-ylmethylene]-*N*-methyl methanaminium hexafluorophosphate. The finished peptides were washed with DCM and were cleaved from the resin using a cocktail of 90% TFA, 5% TIPS and 5% Milli-Q water (%v/v), concentration of the cleavage solution and subsequent precipitation into cold diethyl ether afforded the crude peptides which were purified by preparative HPLC from crude aqueous solutions of peptide dissolved at 10 mg·mL^{-1} and filtered through 0.2 μm filters (TFA = trifluoroacetic acid; TIPS = triisopropylsilane).

Peptide head (P1-6) purification

Preparative scale purification by HPLC was carried out on a Waters UV2489 equipped with a Phenomenex Eclipse XDB-C18 column using MeCN and Milli-Q water (both with 0.1% TFA) as eluents. The column was washed for 5 min with 5% MeCN, followed by gradients of 5% to 65% (**P1-3**) or 5% to 90% (**P4-6**) both over 30 min. Fractions containing the peptide were identified using mass spectrometry, the MeCN was removed from the collected fractions by evaporation and the subsequent aqueous solution were lyophilised.

Synthesis of peptide amphiphiles

As an example, **P1T10** was synthesised by addition of decanal (0.9 mg, 6.2 μM) to **P1** (5 mg, 5.65 μM) in DMSO (1 mL), the solution was shaken and heated to 60 °C until the reaction was confirmed to have gone to completion by LC-MS. The solution was precipitated three times in cold diethyl ether, dissolved in water and lyophilised. The other peptide amphiphiles were synthesised using the same procedure: 1.1 equiv of the peptide tail added to 5 mg of the corresponding peptide head in DMSO.

Self-assembly of peptide amphiphiles

Lyophilised powders of the peptide amphiphiles were dissolved in Milli-Q water at a concentration of 20 mg·mL^{-1}, these solutions were sonicated at 60 °C for a period of 60 min. After sonication, the solutions were mixed with either Tris-HCl buffer (50 mM, pH 7.5) or HEPES buffer (100 mM, pH 7.5), thioflavin (5 μm) was added to allow imaging by fluorescence microscopy and finally the prepared samples were diluted to a concentration of 10 mg·mL^{-1} on a microscope slide for imaging. The slides were sealed with parafilm and placed in a high humidity chamber to prevent evaporation. For samples prepared at a higher ionic strength, NaCl

View Article Online
DOI: 10.1039/C8OB02243G

(100 mM) or NaCl (100 mM) and $MgCl_2$ (10 mM) was added and mixed with the sample on the microscope slide. Diluted solutions were prepared by diluting the 20 $mg \cdot mL^{-1}$ stock solution after sonication, this diluted solution was re-sonicated prior to self-assembly studies.

STEM of peptide amphiphiles

Stock solutions were sonicated at 60 °C for a period of 60 min, cationic peptide amphiphiles were left to self-assemble overnight prior to sample preparation, otherwise the procedure is identical to the anionic amphiphile preparation. Anionic amphiphiles were prepared by adding a 10 μL drop of the sample, under the desired conditions for self-assembly and immediately after sonication, to a carbon-coated copper grid and left for 10 min. Afterwards, the excess solution was wicked away using filter paper and left to dry. The grids were washed three times with Milli-Q water, stained with 2.5% gadolinium acetate tetrahydrate and were left to dry under ambient conditions prior to imaging.

Acknowledgements

This work was partially supported by the Spanish Agencia Estatal de Investigación (AEI) [CTQ2014-59646-R, SAF2017-89890-R], the Xunta de Galicia (ED431G/09, ED431C 2017/25 and 2016-AD031) and the ERDF. I.I. thanks the Spanish AEI for a Juan de la Cierva - Formación fellowship (FJCI-2017-31795). J.M. received a Ramón y Cajal (RYC-2013-13784), an ERC Starting Investigator Grant (DYNAP-677786) and a Young Investigator Grant from the Human Frontier Science Research Program (RGY0066/2017).

References

1 T. Aida, E. W. Meijer and S. I. Stupp, *Science*, 2012, **335**, 813–817.
2 E. Krieg, M. M. C. Bastings, P. Besenius and B. Rybtchinski, *Chem. Rev.*, 2016, **116**, 2414–2477.
3 A. Sorrenti, O. Illa and R. M. Ortuño, *Chem. Soc. Rev.*, 2013, **42**, 8200–8219.
4 I. W. Hamley, *Soft Matter*, 2011, **7**, 4122-4318.
5 A. Méndez-Ardoy, J. R. Granja and J. Montenegro, *Nanoscale Horizons*, 2018, **3**, 391–396.
6 Y. Shi, Y. Hu, G. Ochbaum, R. Lin, R. Bitton, H. Cui and H. S. Azevedo, *Chem. Commun.*, 2017, **53**, 7037–7040.
7 A. Fuertes, M. Juanes, J. R. Granja and J. Montenegro, *Chem. Commun.*, 2017, **53**, 7861–7871.
8 H. Shigemitsu, T. Fujisaku, W. Tanaka, R. Kubota, S. Minami, K. Urayama and I. Hamachi, *Nat. Nanotechnol.*, 2018, **13**, 165–172.
9 S. M. Chin, C. V. Synatschke, S. Liu, R. J. Nap, N. A. Sather, Q. Wang, Z. Álvarez, A. N. Edelbrock, T. Fyrner, L. C. Palmer, I. Szleifer, M. Olvera De La Cruz and S. I. Stupp, *Nat. Commun.*, 2018, **9**, 2395.
10 M. Cuerva, R. García-Fandiño, C. Vázquez-Vázquez, M. A. López-Quintela, J. Montenegro and J. R. Granja, *ACS Nano*, 2015, **9**, 10834–10843.
11 J. Montenegro, C. Vázquez-Vázquez, A. Kalinin, K. E. Geckeler and J. R. Granja, *J. Am. Chem. Soc.*, 2014, **136**, 2484–2491.
12 P. A. Korevaar, C. J. Newcomb, E. W. Meijer and S. I. Stupp, *J. Am. Chem. Soc.*, 2014, **136**, 8540–8543.
13 M. J. Webber, C. J. Newcomb, R. Bitton and S. I. Stupp, *Soft Matter*, 2011, **7**, 9665–9672.
14 L. E. R. O'Leary, J. A. Fallas, E. L. Bakota, M. K. Kang and J. D. Hartgerink, *Nat. Chem.*, 2011, **3**, 821–828.
15 D. Spitzer, L. L. Rodrigues, D. Straßburger, M. Mezger and P. Besenius, *Angew. Chem. Int. Ed.*, 2017, **56**, 15461–15465.
16 H. Frisch, E.-C. Fritz, F. Stricker, L. Schmüser, D. Spitzer, T. Weidner, B. J. Ravoo and P. Besenius, *Angew. Chem. Int. Ed.*, 2016, **128**, 7242–7246.
17 H. Frisch, D. Spitzer, M. Haase, T. Basché, J. Voskuhl and P. Besenius, *Org. Biomol. Chem.*, 2016, **14**, 5574–5579.
18 B. Kemper, L. Zengerling, D. Spitzer, R. Otter, T. Bauer and P. Besenius, *J. Am. Chem. Soc.*, 2018, **140**, 534–537.
19 M. Hatip Koc, G. Cinar Ciftci, S. Baday, V. Castelletto, I. W. Hamley and M. O. Guler, *Langmuir*, 2017, **33**, 7947–7956.
20 P. A. Korevaar, C. J. Newcomb, E. W. Meijer and S. I. Stupp, *J. Am. Chem. Soc.*, 2014, **136**, 8540–8543.
21 A. Iscen and G. C. Schatz, EPL, 2017, **119**, 38002.
22 A. Manandhar, M. Kang, K. Chakraborty, P. K. Tang and S. M. Loverde, *Org. Biomol. Chem.*, 2017, **15**, 7993–8005.
23 O. S. Lee, V. Cho and G. C. Schatz, *Nano Lett.*, 2012, **12**, 4907–4913.
24 V. A. Kumar, N. L. Taylor, S. Shi, B. K. Wang, A. A. Jalan, M. K. Kang, N. C. Wickremasinghe and J. D. Hartgerink, *ACS Nano*, 2015, **9**, 860–868.
25 R. Ni and Y. Chau, *Angew. Chem. Int. Ed.*, 2017, **56**, 9356–9360.
26 V. A. Kumar, S. Shi, B. K. Wang, I. C. Li, A. A. Jalan, B. Sarkar, N. C. Wickremasinghe and J. D. Hartgerink, *J. Am. Chem. Soc.*, 2015, **137**, 4823–4830.
27 N. C. Wickremasinghe, V. A. Kumar and J. D. Hartgerink, *Biomacromolecules*, 2014, **15**, 3587–3595.
28 J. Montenegro, M. R. Ghadiri and J. R. Granja, *Acc. Chem. Res.*, 2013, **46**, 2955–2965.
29 D. Straßburger, N. Stergiou, M. Urschbach, H. Yurugi, D. Spitzer, D. Schollmeyer, E. Schmitt and P. Besenius, *ChemBioChem*, 2018, **19**, 912–916.
30 M. J. Webber, E. A. Appel, E. W. Meijer and R. Langer, *Nat. Mater.*, 2015, **15**, 13–26.

View Article Online
DOI: 10.1039/C8OB02243G

31 M. J. Webber and R. Langer, *Chem. Soc. Rev.*, 2017, **46**, 6600–6620.

32 F. Versluis, J. H., van Esch and R. Eelkema, Adv. Mat., 2016, **28**, 4576–4592

33 R. X. M. Merindol and A. Walther, *Chem. Soc. Rev.*, 2017, **46**, 5588–5619.

34 P. A. Janmey, D. R. Slochower, Y.-H. Wang, Q. Wen and A. Cēbers, *Soft. Matter.*, 2014, **10**, 1439–11.

35 R. Ni and Y. Chau, *J. Am. Chem. Soc.*, 2014, **136**, 17902–17905.

36 M. Goktas, G. Cinar, I. Orujalipoor, S. Ide, A. B. Tekinay and M. O. Guler, *Biomacromolecules*, 2015, **16**, 1247–1258.

37 G. Yu, X. Yan, C. Han and F. Huang, *Chem. Soc. Rev.*, 2013, **42**, 6697–6722.

38 M. Inoue, S. Kaida, S. Nakano, C. Annoni, E. Nakata, T. Konno and T. Morii, *Bioorganic Med. Chem.*, 2014, **22**, 6471–6480.

39 R. M. Capito, H. S. Azevedo, Y. S. Velichko, A. Mata and S. I. Stupp, *Science*, 2008, **319**, 1812–1816.

40 A. M. Hungt and S. I. Stupp, *Nano Lett.*, 2007, **7**, 1165–1171.

41 H. Cui, T. Muraoka, A. G. Cheetham and S. I. Stupp, *Nano Lett.*, 2009, **9**, 945–951.

42 R. Zhang, J. D. Smith, B. N. Allen, J. S. Kramer, M. Schauflinger and B. D. Ulery, *ACS Biomater. Sci. Eng.*, 2018, **4**, 2463–2472

43 J. M. Priegue, I. Lostalé-Seijo, D. Crisan, J. R. Granja, F. Fernández-Trillo and J. Montenegro, *Biomacromolecules*, 2018, **19**, 2638–2649.

44 I. Louzao, R. García-Fandiño and J. Montenegro, *J. Mater. Chem. B*, 2017, **5**, 4426–4434.

45 J. M. Priegue, D. N. Crisan, J. Martínez-Costas, J. R. Granja, F. Fernandez-Trillo and J. Montenegro, *Angew. Chem. Int. Ed.*, 2016, **55**, 7492–7495.

46 I. Lostalé-Seijo, I. Louzao, M. Juanes and J. Montenegro, *Chem. Sci.*, 2017, **8**, 7923–7931.

47 P. Besenius, Y. Goedegebure, M. Driesse, M. Koay, P. H. H. Bomans, A. R. A. Palmans, P. Y. W. Dankers and E. W. Meijer, *Soft Matter*, 2011, **7**, 7980–7983.

48 M. Pazo, H. Fernández-Caro, J. M. Priegue, I. Lostalé-Seijo and J. Montenegro, *Synlett*, 2017, **28**, 924–928.

49 J. Collins, Z. Xiao, M. Müllner and L. A. Connal, *Polym. Chem.*, 2016, **7**, 3812–3826.

50 F. Klepel and B. J. Ravoo, *Org. Biomol. Chem.*, 2017, **15**, 3840–3842.

51 Y. Liu, J. M. Lehn and A. K. H. Hirsch, *Acc. Chem. Res.*, 2017, **50**, 376–386.

52 A. Fuhrmann, R. Göstl, R. Wendt, J. Kötteritzsch, M. D. Hager, U. S. Schubert, K. Brademann-Jock, A. F. Thünemann, U. Nöchel, M. Behl and S. Hecht, *Nat. Commun.*, 2016, **7**, 13623.

53 B. Rieß and J. Boekhoven, *ChemNanoMat*, 2018, 710–719.

54 Y. Shi, Y. Hu, G. Ochbaum, R. Lin, R. Bitton, H. Cui and H. S. Azevedo, *Chem. Commun.*, 2017, **53**, 7037–7040.

55 S. Zhang, M. A. Greenfield, A. Mata, L. C. Palmer, R. Bitton, J. R. Mantei, C. Aparicio, M. O. De La Cruz and S. I. Stupp, *Nat. Mater.*, 2010, **9**, 594–601.

56 J. W. Fredy, A. Méndez-Ardoy, S. Kwangmettatam, D. Bochicchio, B. Matt, M. C. A. Stuart, J. Huskens, N. Katsonis, G. M. Pavan and T. Kudernac, *Proc. Natl. Acad. Sci.*, 2017, **114**, 11850-11855.

57 Y. Song, T. C. T. Michaels, Q. Ma, Z. Liu, H. Yuan, S. Takayama, T. P. J. Knowles and H. C. Shum, *Nat. Commun.*, 2018, **9**, 2110.

58 L. S. Wolfe, M. F. Calabrese, A. Nath, D. V. Blaho, A. D. Miranker, Y. Xiong, *Proc. Natl. Acad. Sci. U.S.A.* 2010, **107**, 16863–16868.

59 G. Xu, X. Liu, P. Liu, D. Pranantyo, K. G. Neoh and E. T. Kang, *Langmuir*, 2017, **33**, 6925–6936.

60 S. E. Paramonov, H. W. Jun and J. D. Hartgerink, *J. Am. Chem. Soc.*, 2006, **128**, 7291–7298.

61 M. Yan, P. L. Lewis and R. N. Shah, *Biofabrication*, DOI:10.1088/1758-5090/aac902.

62 R. Motalleb, E. J. Berns, P. Patel, J. Gold, S. I. Stupp and H. G. Kuhn, *J. Tissue Eng. Regen. Med.*, 2018, **12**, e2123–e2133.

63 M. M. So, N. A. Mansukhani, E. B. Peters, M. S. Albaghdadi, W. Zheng, C. M. Rubert Pérez, M. R. Kibbe and S. I. Stupp, *Adv. Biosyst.*, 2018, **2**, 1700123.

View Article Online
DOI: 10.1039/C8OB02243G

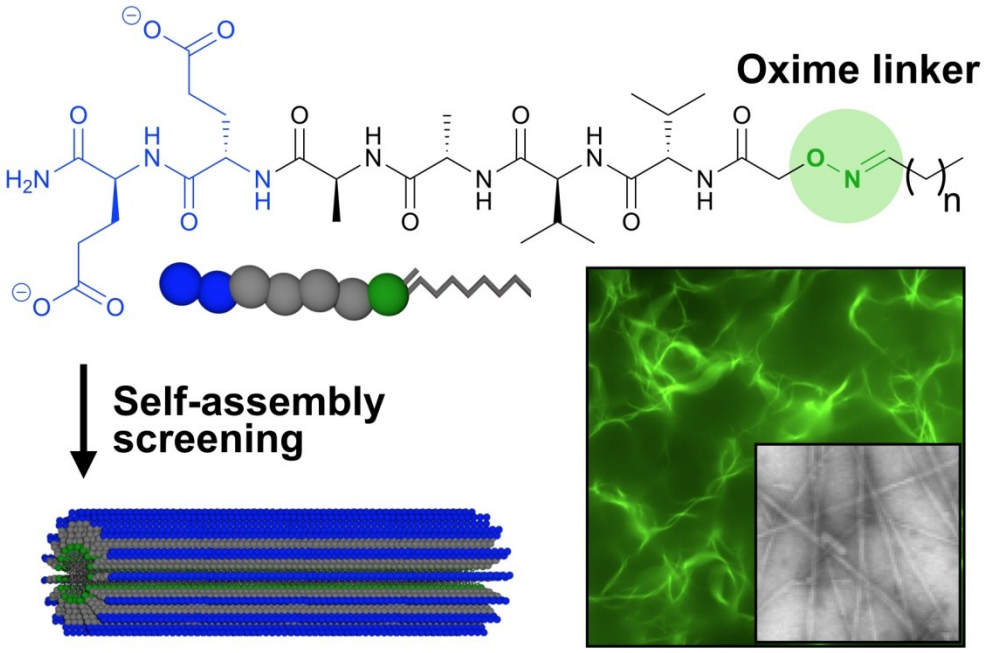

609x408mm (72 x 72 DPI)